RSC Advances

PAPER

View Article Online
View Journal | View Issue

Check for updates

Cite this: *RSC Adv.*, 2022, **12**, 30104

Novel β-cyclodextrin doped carbon dots for host–guest recognition-assisted sensing of isoniazid and cell imaging

Lu-Shuang Li,[a] Ying-Xia Zhang,[a] Wei Gong*[b] and Jing Li *[b]

Received 14th August 2022
Accepted 13th October 2022

DOI: 10.1039/d2ra05089g

rsc.li/rsc-advances

In the present study, novel β-cyclodextrin doped carbon dots (CCDs) were prepared *via* a simple one-pot hydrothermal method at a mild temperature (140 °C), using mixtures of β-cyclodextrin and citric acid as precursors. By characterizing the chemical properties of CCDs prepared at 140 °C and 180 °C, the importance of low-temperature reaction for preservation of the specific structure of β-CD was elucidated. The CCDs showed excellent optical properties and were stable to changes in pH, ionic strength and light irradiation. Since the fluorescence of the CCDs could be selectively quenched by isoniazid (INZ) through specific host–guest recognition effects, a convenient isoniazid fluorescence sensor was developed. Under the optimal conditions, the sensor exhibited a relatively low detection limit of 0.140 μg mL^{-1} and a wide detection range from 0.2 μg mL^{-1} to 50 μg mL^{-1} for INZ detection. Furthermore, the sensor was employed successfully for the determination of INZ in urine samples with satisfactory recovery (91.1–109.5%), displaying potential in clinical applications. Finally, low cytotoxicity of the prepared CCDs was confirmed using the CCK-8 method, followed by application in HepG2 cell imaging.

Open Access Article. Published on 21 October 2022. Downloaded on 10/3/2024 7:25:47 AM.
This article is licensed under a Creative Commons Attribution-NonCommercial 3.0 Unported Licence.

1 Introduction

Tuberculosis is a chronic infectious disease caused by Mycobacterium. Owing to the selective and strong antibacterial effect against Mycobacterium infection, isoniazid (INZ) is often chosen as the preferred treatment for tuberculosis, administered in combination with other drugs.[1,2] However, there exists a very fine margin separating therapeutic and lethal dosages. Considering the wide differences in response to treatments across individuals, it is necessary to adjust the dosage of INZ administered by accounting for the INZ content already in the individuals' bodies.[3,4] The commonly-used methods for INZ determination include photometric analysis, electrochemiluminescence analysis, high performance liquid chromatography (HPLC) analysis and so on.[1–3] However, these methods usually require complicated sample pre-treatments, expensive instrument and well-trained operators. This implies that the development of a detection method which provides quick response, simple operation and high sensitivity is of great significance.

In recent years, fluorescent assays have attracted considerable attention with merits of simplicity, rapid response, high selectivity and sensitivity.[5] Compared to conventional fluorescent materials, such as organic fluorescent dyes, metal nanoclusters and quantum dots, carbon dots (CDs) are perceived to be promising nanomaterials for the construction of fluorescent sensors,[6,7] given their excellent fluorescence performance, easy preparation, high water-solubility, chemical inertness, good photostability and low cytotoxicity.[8–12] So far, CDs based sensors have been successfully applied in the analysis of various compounds.[13–20] However, as there are no specific functional groups on the surface of CDs, many fluorescence sensing platforms based on them show constraints of low selectivity and poor anti-interference. As such, intensive effort has been devoted to synthesizing CDs with specific heteroatom or functional groups through doping or post modification to achieve selective interactions.[21–25]

β-Cyclodextrin (β-CD) is a cyclic oligosaccharide composed of seven D-galactose units linked by α-1,4-glycosidic bonds thus obtaining a hydrophilic outer surface and a hydrophobic inner cavity. The unique molecular structure of β-CD allows some compounds to enter the cavity completely or partially and form host–guest inclusion complexes, which has been proved to be effective for constructing highly selective fluorescence sensors in several studies.[26–30] Cayuela *et al.* prepared β-CD modified carbon dots with multi-walled carbon nanotubes to achieve selective detection of C_{60}.[31] Tang *et al.* used activated carbon to prepare and modify the carbon dots with β-CD, which led to specific recognition of *p*-nitrophenol.[32] Luo *et al.* prepared β-CD modified carbon dots using carbonic acid and L-cysteine for the detection of testosterone.[27] Although β-CD has been employed as a recognition molecule in all the above CDs-based sensors, the detection targets varied. It is postulated that the selectivity

[a]*Key Laboratory of Tropical Biological Resources of Ministry of Education, School of Pharmaceutical Sciences, Hainan University, Haikou 570228, China*
[b]*Xiangyang Central Hospital, Affiliated Hospital of Hubei University of Arts & Science, Xiangyang 441021, China. E-mail: Lijing@hbuas.edu.cn; gongzhewei@sina.com*

© 2022 The Author(s). Published by the Royal Society of Chemistry

Open Access Article. Published on 21 October 2022. Downloaded on 10/3/2024 7:25:47 AM.
This article is licensed under a Creative Commons Attribution-NonCommercial 3.0 Unported Licence.

of a sensor is decided by the properties of CDs and β-CD together. In addition, CDs were always synthesized first and then modified with β-CD to retain its recognition ability in previous studies, thus resulting in complicated preparation and purification processes.[29,33–35] Therefore, the exploration of new methods of CDs preparation and β-CD modification to simplify the construction of new fluorescence sensors is necessary.

It has been demonstrated that the inclusion complexes of β-CD and INZ can be formed *via* host–guest reaction.[36–38] Inspired by this, we initiated a scheme to construct a selective fluorescence sensor for INZ by combining CDs and β-CD. In this work, carbon dots were prepared with β-CD and citric acid as precursors and named as CCDs, by one-pot hydrothermal method performed at a relatively low temperature (140 °C) to preserve the specific structure of β-CD. The fluorescence of CCDs was extremely stable and can be selectively quenched by INZ through the synergy of static and dynamic quenching mechanisms. The INZ fluorescence sensor was constructed with a limit of detection (LOD) of 0.140 μg mL^{-1} and was successfully applied in the detection of actual urine samples with recoveries in the range of 91.1–109.5%. Additionally, the CCDs showed relatively low cytotoxicity and were successfully applied in HepG2 cell imaging.

2 Experimental

2.1 Chemicals and reagents

Citric acid and isoniazid (INZ) were purchased from Aladdin Chemical Reagent Co., Ltd. (Shanghai, China). β-Cyclodextrin (β-CD) was obtained from Tokyo Chemical Industry (Tokyo, Japan). Uric acid, urea, glucose, HCl, NaCl, KCl, NH_4Cl, $MgCl_2$, $NaHCO_3$, $Ca(NO_3)_2 \cdot 4H_2O$ and NaOH were purchased from Sinopharm Chemical Reagent Co., Ltd. (Shanghai, China). Ultrapure water was prepared by Heal Fore NW system (Shanghai, China). Blank urine was collected from healthy volunteers who were not exposed to INZ before.

2.2 Instruments

Transmission electron microscopy (TEM) image was taken on a JEM-2100 microscope (JEOL, Japan). Fourier transform infrared (FTIR) spectrum was recorded on an AVATAR 360 spectrometer (Thermo, USA). X-ray photoelectron spectroscopy (XPS) spectra were obtained on an ESCALAB 250Xi electron spectrometer (Thermo, USA). Ultraviolet-visible (UV-vis) absorption spectra and fluorescence (FL) spectra were recorded on a Lambda 365 UV-vis spectrophotometer (PerkinElmer, USA) and an F-4600 fluorescence spectrophotometer (Hitachi, Japan), respectively.

2.3 Preparation of CCDs

CCDs were synthesized *via* a facile one-pot hydrothermal method. In detail, 0.50 g β-CD and 1.50 g citric acid were dissolved in 10 mL ultrapure water. Then the mixture was sealed in a 25 mL Teflon-lined stainless steel and reacted in an oven at 140 °C for 12 h. After cooling down to room temperature naturally, the product was dialyzed against ultrapure water in a dialysis bag (1000 MWCO) to remove unreacted small molecules. The solvent of the resulting solution was removed by rotary evaporation and the CCDs solid was obtained by freeze-drying.

2.4 Optical properties of CCDs

The optical properties of CCDs were studied by UV-vis and fluorescence analysis. The fluorescence intensity of CCDs solutions at different pH (1–10) adjusted with a small volume of HCl or NaOH solution and in presence of different concentrations (0–1.0 M) of NaCl was measured to evaluate the pH and ionic strength stability. The CCDs solution was continuously irradiated with ultraviolet of 370 nm for 7200 s, and the fluorescence intensity of the solution was monitored constantly to investigate the photostability of CCDs. Fluorescence intensity measurements were all carried out at excitation and emission wavelength of 370 nm and 530 nm, respectively.

2.5 Detection of INZ by CCDs

A known amount of INZ was dissolved in ultrapure water to obtain the stock solution. Standard series working solutions of INZ (0, 0.2 μg mL^{-1}, 0.5 μg mL^{-1}, 1 μg mL^{-1}, 2 μg mL^{-1}, 5 μg mL^{-1}, 10 μg mL^{-1}, 20 μg mL^{-1}, 50 μg mL^{-1}) were prepared by dilution of stock solution with ultrapure water.

The detection conditions were optimized in terms of the pH and incubation reaction time. For a typical detecting process, the pH of the standard working solution or samples was adjusted to a specific pH with a small volume of HCl or NaOH solution. 50 μL CCDs solution (80 μg mL^{-1}) was added to 2 mL working solution prepared above. After vortexing and incubating at room temperature for a known period of time, the mixture was subjected to the fluorescence intensity measurement. The quenching efficiency (F_0/F) was calculated, where F and F_0 are the fluorescence intensity of solution with and without INZ, respectively.

To evaluate the selectivity, the influence of ions (Na^+, Cl^-, K^+, NH_4^+, HCO_3^-, Mg^{2+}) and small chemicals (urea, uric acid and glucose) at concentrations of 10 μM and 20 μg mL^{-1}, respectively, on the fluorescence intensity of CCDs were investigated separately. In addition, each of the mentioned substances was separately introduced into the INZ (20 μg mL^{-1}) working solution to investigate the coexisting interference of them.

2.6 Real sample analysis

Urine sample from a healthy volunteer was first filtered through a 0.22 μm filter before measurement. All experiments were performed in accordance with the guidelines of Declaration of Helsinki, and approved by the ethics committee at Xiangyang Central Hospital (affiliated hospital of Hubei University of Arts & Science) with a waiver of Informed Consent. Standard urine samples spiked with a series of INZ concentration (0, 0.2 μg mL^{-1}, 0.5 μg mL^{-1}, 1 μg mL^{-1}, 2 μg mL^{-1}, 5 μg mL^{-1}, 10 μg mL^{-1}, 20 μg mL^{-1}, 50 μg mL^{-1}) were prepared by diluting stock solution with blank urine. The recovery assay was performed by monitoring spiked urine samples with known INZ

Open Access Article. Published on 21 October 2022. Downloaded on 10/3/2024 7:25:47 AM. This article is licensed under a Creative Commons Attribution-NonCommercial 3.0 Unported Licence.

concentrations (2 μg mL^{-1}, 20 μg mL^{-1}, 80 μg mL^{-1}). The recovery was calculated by the following eqn (1),

$$\text{Recovery } (\%) = (C_{\text{measured}}/C_{\text{added}}) \times 100\% \quad (1)$$

where C_{measured} is the INZ concentration tested with the constructed sensor, and C_{added} is the actual added concentration of INZ.

2.7 Cytotoxicity test and cell imaging

HepG2 cells were resuscitated in a 6-well culture plate with a cover glass in Dulbecco's modified Eagle's medium (DMEM) complete medium containing 10% fetal bovine serum and 1% penicillin–streptomycin. HepG2 cells were cultured at 37 °C and 5% CO_2 for 24 h. Then the medium was discarded, and a fresh medium containing CDs (100 μg mL^{-1}) was added. After 2 h culturing, the medium was discarded, and the cover glass was placed in cold acetone for 10 min to fix the cells. The cells were washed with PBS to remove free or physically adsorbed CCDs. Thereafter, the labelled cells were observed and fluorescence images were taken by a confocal microscopy (Olympus FV1200, Japan).

CCK-8 method was used to assess the cytotoxicity of the CCDs with 1% (v/v) DMSO as positive control. 100 μL HepG2 cell suspension (5×10^4 mL^{-1}) was added to each well of a 96-well plate, and cultured in DMEM medium for 24 h. Then, the culture medium was discarded and medium with different concentrations of CCDs (0, 5 μg mL^{-1}, 10 μg mL^{-1}, 50 μg mL^{-1}, 100 μg mL^{-1}, 200 μg mL^{-1}) were added. After culturing for another 24 h, the medium was removed and replaced with 100 μL PBS. 10 μL CCK-8 solution (BioSharp, Hefei, Anhui) was added to each well and incubated for 1 h. The absorbance at 450 nm was measured by a microplate reader (Multiskan Sky-High, Thermo Fisher, USA). The cell viability was calculated by the following eqn (2),

$$\text{Cell viability } (\%) = (A/A_{\text{control}}) \times 100\% \quad (2)$$

where A and A_{control} represented the absorbance values of the wells from the experimental group and negative control group, respectively.

3 Results and discussion

3.1 Preparation of CCDs

There are many available methods for preparing CDs and researchers are still devoted to developing new approaches. Even so, hydrothermal technique is still one of the most frequently-used method, citing reasons such as ease of operation and no requirement of special instruments and chemicals. As reported, in order to pursue an excellent fluorescence performance for CDs, a high reaction temperature in excess of 180 °C is usually employed.[39,40] Under this reaction condition, CDs were produced through polymerization and carbonization, but the high temperature may destroy the particular functional groups on the carbon precursor to a large extent, thus resulting in a lack of specificity of CDs-based sensors.[7,41] In this work, β-CD was selected as the doping substance and directly introduced into the reaction system to prepare CDs with specific recognition site. For the sake of retaining the specific recognition structure of β-CD and enhancing the fluorescence performance of CCDs, the reaction conditions, including reaction temperature, the composition of carbon sources and reaction time, were optimized respectively.

The hydrothermal products under different conditions were diluted with ultra-pure water in equal parts, and their fluorescence spectra were scanned to evaluate the fluorescence properties of CCDs. As shown in Fig. 1a, the shapes of the fluorescence spectra with reaction temperature under 160 °C were almost the same, obtaining two peaks at around 445 nm and 525 nm, and the fluorescence intensity enhanced markedly with the increase of temperature from 120 °C to 140 °C. When the reaction temperature was increased to 180 °C, the fluorescence intensity at 445 nm was greatly enhanced and the shape of the fluorescence spectrum changed significantly. We hypothesized that the reactions and the products in the system were quite different from those at lower temperature. According to previous studies, high temperature may cause extreme carbonation and most specific functional groups may be destroyed.[7,8,41] In addition, we also investigated the effect of reaction temperature on the size of CCDs. The TEM images of CCDs prepared at different temperatures were taken (Fig. 2a and d–f). As demonstrated in Fig. 2b, the higher of the

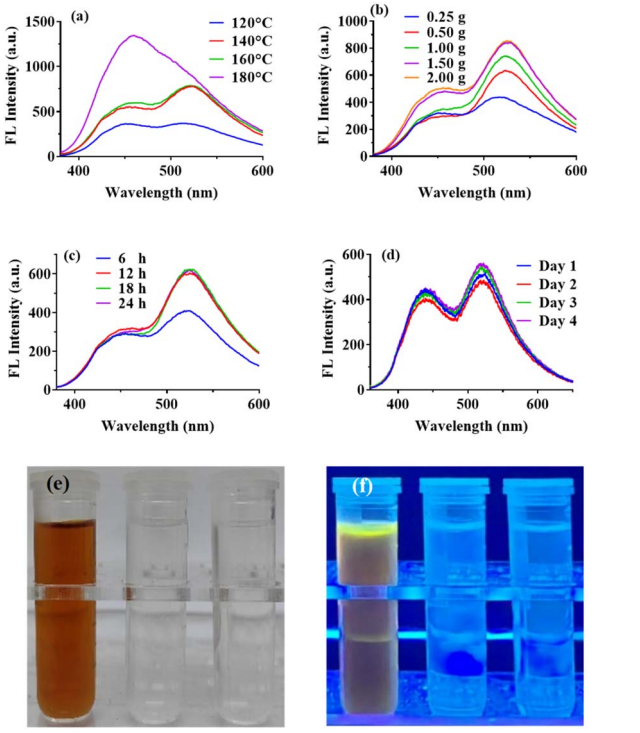

Fig. 1 The influences of hydrothermal temperature (a), the amount of citric acid (b), and hydrothermal time (c) on the fluorescence of CCDs. (d) Fluorescence spectra of CCDs prepared in four consecutive days. Hydrothermal reaction product with different sources (from left to right: β-CD and citric acid, β-CD, citric acid) under daylight (e) and UV light (f).

© 2022 The Author(s). Published by the Royal Society of Chemistry

Open Access Article. Published on 21 October 2022. Downloaded on 10/3/2024 7:25:47 AM.
This article is licensed under a Creative Commons Attribution-NonCommercial 3.0 Unported Licence.

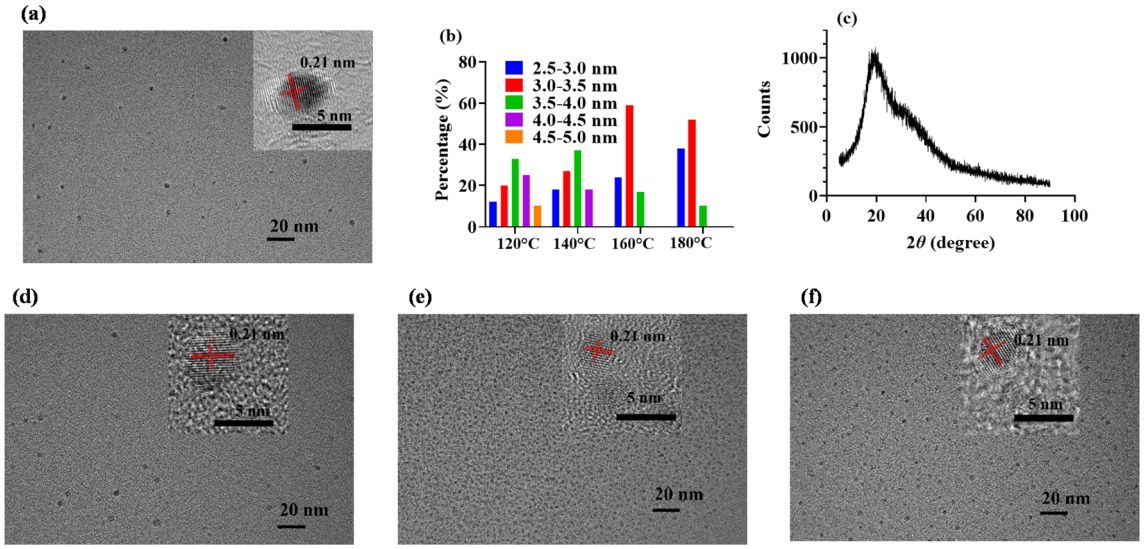

Fig. 2 TEM images of CCDs prepared at 140 °C (a), 120 °C (d), 160 °C (e) and 180 °C (f). (b) Size distribution of CCDs prepared at different temperature. (c) XRD spectrum of CCDs prepared at 140 °C.

temperature, the more concentrated of the size distribution of CCDs. In addition, the average diameters were calculated to be 3.76 nm, 3.51 nm, 3.22 nm and 3.11 nm for CCDs prepared at 120 °C, 140 °C, 160 °C and 180 °C, respectively. Though the diameters of these CCDs only varied a little, the phenomenon of the higher of the reaction temperature, the smaller the particle size of CDs was observed, demonstrating the reaction temperature may have an influence on the size of CCDs. To optimize the fluorescence intensity while retaining the functional groups, 140 °C was selected for the subsequent experiments. As shown in Fig. 1b, the fluorescence intensity of CCDs solution gradually rose with the increase in the amount of citric acid added into the reaction system, and eventually reached maximum at 1.50 g. Citric acid added in excess may unnecessarily lengthen the purification time, hence the amount of citric acid was fixed at 1.50 g. According to the experimental results obtained from optimizing the reaction time, 12 h was sufficient to ensure complete reaction of the system (Fig. 1c). In summary, the optimal condition for the preparation of CCDs was 0.50 g β-CD and 1.5 g citric acid dissolved in 10 mL water and reacted at 140 °C for 12 h. For verifying the reproducibility of the preparation method, CCDs were repeatedly prepared for 4 consecutive days. As shown in Fig. 1d, the fluorescence spectra of these CCDs almost entirely overlapped, indicating that the constructed preparation method was repeatable.

To conform the formation of β-CD doped carbon dots, β-CD and citric acid were separately used as reactants for hydrothermal reaction under the same conditions (140 °C for 12 h) to rule out the possibility of a mixture of two different fluorophores obtained from two different sources. As observed in Fig. 1e and f, in the presence of only one carbon source, no obvious color change or fluorescence of the reaction system was observed after the reaction, demonstrating no fluorophore was obtained. Same as other reports, carbon dots derived from citric acid usually need higher temperature (exceed 180 °C). While, with β-CD and citric acid together in the system, the obtained product showed claybank under daylight and yellow fluorescence under UV light, confirming the formation of CCDs. According to this result, CCDs can only be obtained with both citric acid and β-CD in the reaction system, which was not a mixture of two different fluorophores.

3.2 Characterization of CCDs

The morphology of CCDs was first characterized. As shown in Fig. 2a, the TEM image revealed that the prepared CCDs were quasi spherical and well monodispersed in aqueous solution. As shown in the insert, high resolution TEM image showed a clear lattice spacing of 0.21 nm, which can be attributed to the in-plane lattice spacing of graphene structure.[42] The diameter of CCDs was in a narrow distribution between 2.5 nm and 4.5 nm (Fig. 2b). XRD analysis was performed to investigate the crystalline structure of CCDs. The XRD pattern of the CCDs showed a broad diffraction peak at 23° of the 2θ value (Fig. 2c), indicating that the prepared CCDs have good crystallinity,[7] which is consistent with the TEM results.

The surface functional groups and elemental composition of CCDs were investigated through FTIR and XPS. According to previous studies, the temperature of hydrothermal reaction for preparation of CDs was usually higher than 180 °C.[5,7] We suspect that high temperature may cause extreme carbonation and destruction of specific functional groups. To verify the importance of low temperature reaction to preserve the specific structure of β-CD on the surface of CCDs, CCDs prepared at 140 °C (CCDs-140) and 180 °C (CCDs-180) were compared. As displayed in Fig. 3, the FTIR spectra of β-CD and CCDs-140 were very similar, showing that CCDs-140 had similar functional groups as β-CD. The characteristic absorption peaks at 3400 cm^{-1}, 2920 cm^{-1}, 1640 cm^{-1}, 1400 cm^{-1} and 1040 cm^{-1} can be associated with the O–H, C–H, C=O/C=C, C–H, C–O groups respectively.[35,42] The only peak observed at 1730 cm^{-1} in

Open Access Article. Published on 21 October 2022. Downloaded on 10/3/2024 7:25:47 AM.
This article is licensed under a Creative Commons Attribution-NonCommercial 3.0 Unported Licence.

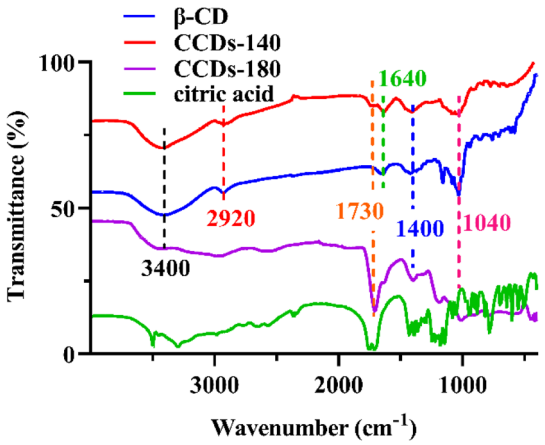

Fig. 3 FTIR spectra of CCDs.

the spectrum of CCDs-140 was the characteristic absorption of C=O,[7] proving the participation of citric acid in the formation of CCDs. While the spectrum of CCDs-180 was very different from that of β-CD and CCDs, the results showed that the chemical structure of the carbon source changed significantly at high reaction temperature, further reaffirming our speculation that the functional groups, to a large extent, can be preserved under low reaction temperature.

As shown in Fig. 4a and b, the XPS full-scan spectra of both CCDs-140 and CCDs-180 showed two peaks, which corresponded to the binding energy of C 1s and O 1s. The element analysis of the XPS peak revealed that the CCDs-140 contained C and O at the percentage of 55.13%, 42.89%, and the CCDs-180 contained C and O at the percentage of 55.37%, 43.34%. The above results demonstrated that the element composition of CCDs prepared under the two temperature reaction conditions were basically the same. To further investigate the differences in the surface functional groups of the two CCDs, high-resolution XPS spectra were performed. In Fig. 4c, three peaks corresponding to the binding energy of 284.58 eV, 286.28 eV, 288.73 eV were found in C 1s spectrum of CCDs-140, and were ascribed to C–C/C=C, C–O and C=O bonds,[31,42] respectively. The O 1s spectrum of CCDs-140 (Fig. 4e) comprised of two peaks: 531.83 eV (C=O) and 533.03 eV (C–O).[8,17] As for CCDs-180, the C 1s spectrum depicted in Fig. 4d, was made up of three peaks at 284.68 eV, 286.08 eV and 288.83 eV, which were ascribed to C–C/C=C, C–O and C=O bonds,[13,42] respectively. The O 1s spectrum of CCDs-180 can be decomposed into two sub-peaks at 531.83 eV and 533.03 eV, corresponding to C=O and C–O,[8,17] respectively (Fig. 4f).

Collectively, the results of FTIR and XPS analysis demonstrated that hydrophilic functional groups (–OH, –COOH, *etc.*) existed on the surface of both CCDs-140 and CCDs-180, which accounted for their excellent water solubility. The specific composition of the functional groups on the two CCDs was quite different. The β-CD-like structure was only present on CCDs-140, thus providing selective sites for sensing applications. This further verified the importance of performing the reaction at mild temperature. Only CCDs-140 was applied in the following experiments.

3.3 Optical properties of CCDs

The optical properties of CCDs were investigated using UV-vis and fluorescence spectrophotometer. As shown in Fig. 5a, prior to hydrothermal reaction, no observable peak could be found in the absorption spectrum of the reaction system (red line). The green line illustrated the UV-vis absorption curve of CCDs in aqueous solution. A peak was clearly observed at 280 nm, which may be attributed to the n–π* transition of functional groups present on the CCDs,[8,21,42] proving that the carbon sources had undergone chemical reaction. The aqueous

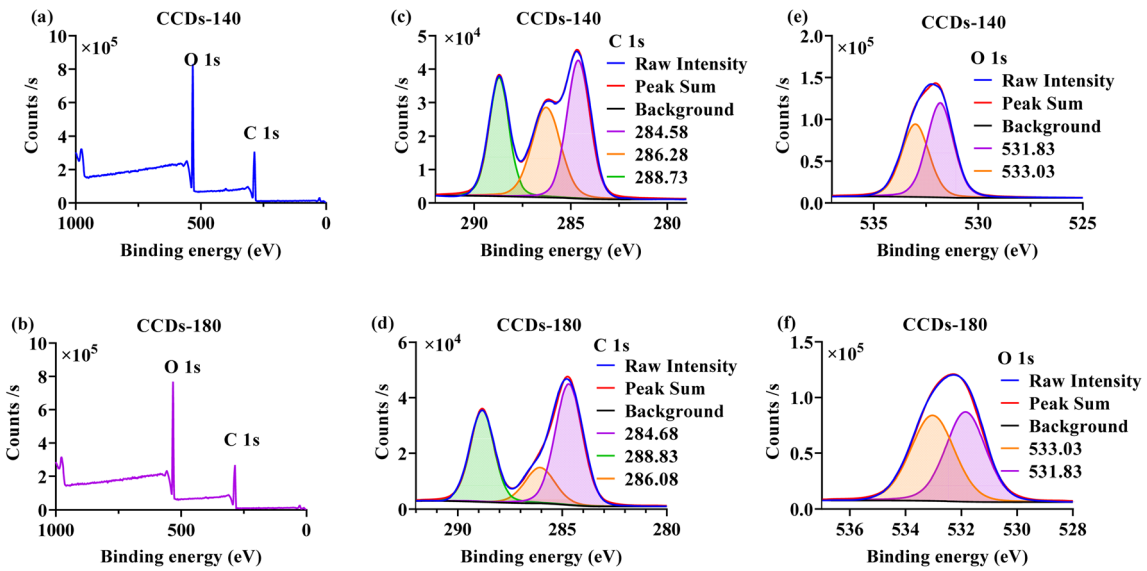

Fig. 4 Full scan XPS spectra of CCDs-140 (a) and CCDs-180 (b). High resolution spectra of C 1s of CCDs-140 (c) and CCDs-180 (d). High resolution spectra of O 1s of CCDs-140 (e) and CCDs-180 (f).

© 2022 The Author(s). Published by the Royal Society of Chemistry

Open Access Article. Published on 21 October 2022. Downloaded on 10/3/2024 7:25:47 AM.
This article is licensed under a Creative Commons Attribution-NonCommercial 3.0 Unported Licence.

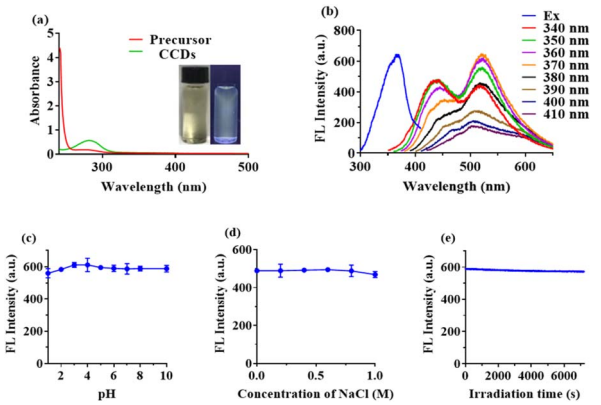

Fig. 5 (a) UV-vis absorption spectra of CCDs and the precursor solution. (b) Excitation (Em = 530 nm) and emission spectra of CCDs. (c) Effect of pH on the fluorescence intensity of CCDs. (d) Effect of ionic strength on the fluorescence intensity of CCDs. (e) Photostability of CCDs.

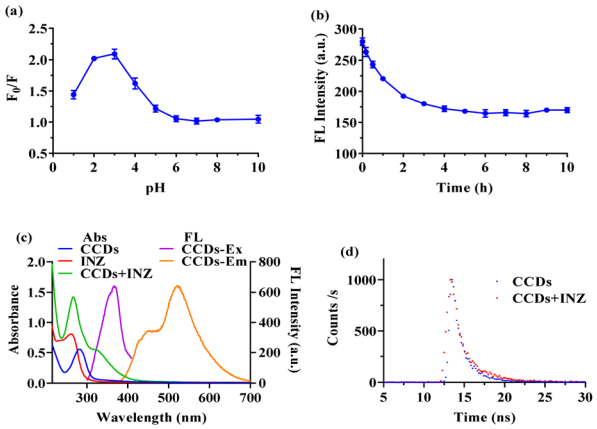

Fig. 6 Influence of (a) pH and (b) reaction time on fluorescence quenching. (c) UV-vis absorption spectra (Abs) of CCDs, INZ and the mixture of them and the excitation (Ex) and emission (Em) fluorescence spectra (FL) of CCDs. (d) The fluorescence lifetime decay curves of the CCDs with and without INZ.

solutions of CCDs were pale yellow when observed under sunlight, and emit yellow green fluorescence under ultraviolet light of 365 nm (inset in Fig. 5a).

The excitation and emission spectra of CCDs with different excitation wavelengths were presented in Fig. 5b. As observed, the spectra of CCDs covered a wide range of wavelength, which was not a simple single peak, but an irregular shape. This phenomenon was also presented in many previous studies.[43,44] Many researches have shown that the fluorescence of CDs may be generated by the carbogenic core or surface functional groups.[45,46] Therefore, the different sizes of CCDs or the presence of multiple functional groups on the surface may be responsible for the multiband emission properties. The spectra of CCDs covered a wide range of wavelength and the highest fluorescence intensity was observed at excitation and emission wavelengths of 370 nm and 530 nm, respectively. The fluorescence stability of the synthesized CCDs was studied with respect to pH, ionic strength and irradiation. As shown in Fig. 5c, the fluorescence intensity of CCDs remained nearly unchanged over a wide pH range (1–10). The existence of NaCl had little effect on the fluorescence intensity of CCDs, even at a relative high concentration of 1 M (Fig. 5d). When the CCDs solution was continuously irradiated with UV light of 370 nm, the fluorescence intensity did not decrease significantly, indicating good photo stability (Fig. 5e).

3.4 Detection of INZ by CCDs

3.4.1 Optimization of fluorescence sensing conditions. In the preliminary experiments, the fluorescence of CCDs was found to be quenched in the presence of INZ, as expected. This hence suggested that it is feasible to construct an INZ sensor with CCDs. The pH value and reaction time were optimized to improve the sensitivity. As shown in Fig. 6a, the pH of the system had a great influence on the fluorescence quenching efficiency. In neutral or alkaline condition (pH 7–10), INZ can hardly quench the fluorescence of the CCDs. With the pH decrease from 6 to 3, the quenching efficiency gradually increased, implying that acidic condition was essential for the interaction between INZ and the functional groups on CCDs. However, if the pH got too low, a dramatic decrease of the quenching efficiency was observed which might be attributed to the partially destruction of the β-CD-like structure on the surface of CCDs thus resulting in a decrease of available reaction sites with INZ.[47] According to the results of from the fluorescence stability investigation in Section 3.3, the fluorescence of CCDs remained relatively stable even under strong acidic condition. To sum up, we can presume that the β-CD-like structure on the surface was not the main fluorescent emitting group. Then the reaction time for detection was evaluated sequentially under the optimal pH of 3. As shown in Fig. 6b, when CCDs were added to the solution of INZ, the fluorescence intensity of CCDs gradually decreased and remained stable still after 6 h, which was applied in the following sensing experiments. The response time was much longer than the previously constructed CDs fluorescence sensors. This phenomenon may have been caused by the slow interaction between INZ and CCDs, reaffirming the host–guest inclusion reaction mechanism.

3.4.2 Sensing mechanism. The INZ sensing mechanism with CCDs was investigated through spectral and fluorescence lifetime analysis. As shown in Fig. 6c, there is little overlap between the fluorescence spectra of CCDs and the absorption spectrum of INZ, thus ruling out FRET or IFE quenching mechanisms.[48–50] Compared to the UV-vis spectra of CCDs and INZ individually, a new absorption shoulder peak was observed in the spectrum of the mixed solution at around 320 nm (Fig. 6c), indicating the occurrence of chemical reaction between CCDs and INZ and the static quenching mechanism.[48–50] The fluorescence lifetimes of CCDs were calculated to be 1.69 ns with two decay components of 1.01 ns (59.88%) and 2.71 ns (40.12%) (Fig. 6d). The fluorescence lifetimes of CCDs in the presence of INZ were calculated to be 2.40 ns, containing two decay components, *i.e.* 1.36 ns (69.19%) and

Open Access Article. Published on 21 October 2022. Downloaded on 10/3/2024 7:25:47 AM.
This article is licensed under a Creative Commons Attribution-NonCommercial 3.0 Unported Licence.

4.73 ns (30.81%) (Fig. 6d). The decrease in average lifetime decay of CCDs suggested the possible existence of a dynamic quenching mechanism.[48–50] In summary, the introduction of INZ into CCDs solution may lead to the selective host–guest interaction between them and the fluorescence of the CCDs was quenched through the synergy of static and dynamic quenching mechanisms.

3.4.3 Analysis performances of INZ sensor. The selectivity and anti-interference ability of the proposed INZ sensor based on CCDs was evaluated. As can be seen in Fig. 7a,the fluorescence of CCDs was inhibited by the presence of INZ, and the possible interfering substances in the urine, including common ions (Na^+, K^+, Ca^{2+}, Mg^{2+}, NH^{4+}, Cl^-, HCO_3^-) and chemicals (urea, uric acid and glucose) had little effect on the fluorescence of CCDs (Fig. 7a, blue bar). In addition, the coexistence of these substances showed no interference on the detection of INZ (Fig. 7a, red bar), which implied that the method has high selectivity and strong anti-interference ability. Fig. 7b shows the fluorescence spectra of CCDs in the presence of different concentrations of INZ in ultrapure water matrix. It could be seen that the fluorescence of CCDs gradually decreased as the concentration of INZ increased. A good linear relationship between F_0/F and INZ concentration in the range of 0.2–50 μg mL^{-1} (1.46–364.59 μM) was obtained (Fig. 7c). The limit of detection (LOD) for INZ was calculated to be approximately 0.140 μg mL^{-1} (1.02 μM) at the signal to noise (S/N) of 3.

3.4.4 Detection of INZ in urine samples. The feasibility of the method in the detection of actual urine samples was validated by investigating the linear relationship between F_0/F and the concentration of INZ in urine matrix. Fig. 7d showed the fluorescence spectra of CCDs in urine with the presence of INZ at different concentrations. Under the influence of urine matrix, the fluorescence spectra of CCDs were somewhat different from the ultrapure water matrix, but the fluorescence intensity of CCDs was still gradually quenched as INZ concentration increased, demonstrating that the matrix did not affect the specific response of CCDs to INZ. As shown in Fig. 7e, the relationship between F_0/F and the concentration of INZ was still linear in the spiked concentration range of 0.2–50 μg mL^{-1} (1.46–364.59 μM). Therefore, the method showed practical applications in the detection of INZ in urine. The LOD was calculated to be 0.143 μg mL^{-1} (1.04 μM), which was comparable to the value from the ultrapure water matrix.

As depicted in Table 1, analysis of spiked urine samples demonstrated recovery percentage in the range of 91.1% to 109.5%, substantiating the accuracy of the method and compared to the INZ fluorescent sensors based on CDs from previous reports (Table 2), the proposed method had comparable or better sensing performance (linear range and LOD).

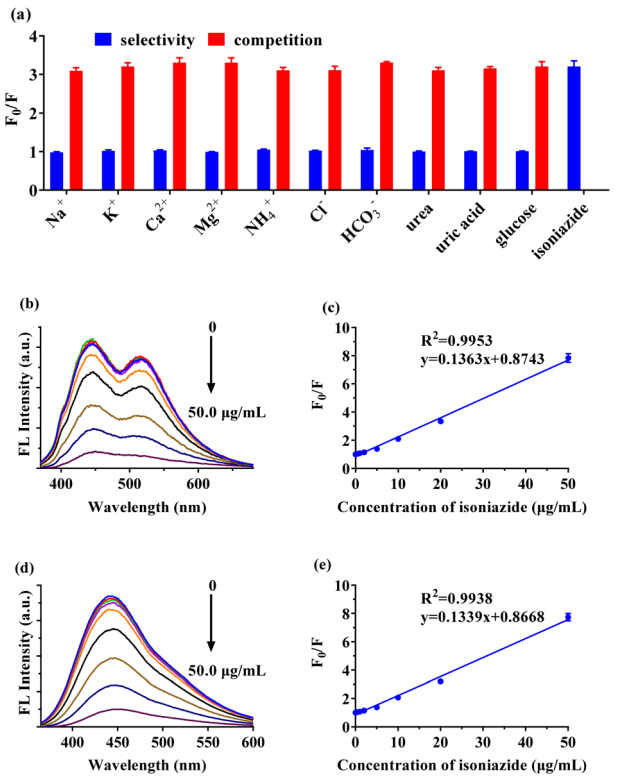

Fig. 7 (a) Selectivity and coexistence interference (competition) in the detection of INZ by CCDs. (b) Fluorescence spectra of CCDs in ultrapure water matrix with different concentrations of INZ at excitation wavelength of 340 nm. (c) The linear plot of F_0/F *versus* concentration of INZ in ultrapure water matrix. (d) Fluorescence spectra of CCDs in urine matrix with different concentrations of INZ at excitation wavelength of 340 nm. (e) The linear plot of F_0/F *versus* concentration of INZ in urine matrix.

3.5 Cytotoxicity and cell imaging

Carbon dots are often used as biomarkers owing to their good biocompatibility and low toxicity.[7,8] The cytotoxicity of the

Table 1 Recovery test of INZ in urine samples

Sample	Added (μg mL^{-1})	Measured (μg mL^{-1})	Recovery (%)	RSD ($n = 3$) (%)
1	2.00	2.19	109.5	3.7
2	10.00	9.11	91.1	1.4
3	50.00	51.40	102.8	3.9

Table 2 Comparison of CCDs sensor with other CDs sensors for INZ detection

Sensors	Carbon source	Synthetic temperature (°C)	LOD (μM)	Linear range (μM)	Ref.
FCDs	Folic acid	225	1.15	4.0–140	3
S,N-CDs	L-Cysteine and citric acid monohydrate	200	0.28	0.5–5	4
N-CDs	Liu-bao tea and ethylene diamine	180	0.7	2.0–120.0	2
CCDs	β-Cyclodextrin and citric acid	140	1.02	1.46–364.59	This work

© 2022 The Author(s). Published by the Royal Society of Chemistry

Open Access Article. Published on 21 October 2022. Downloaded on 10/3/2024 7:25:47 AM.
This article is licensed under a Creative Commons Attribution-NonCommercial 3.0 Unported Licence.

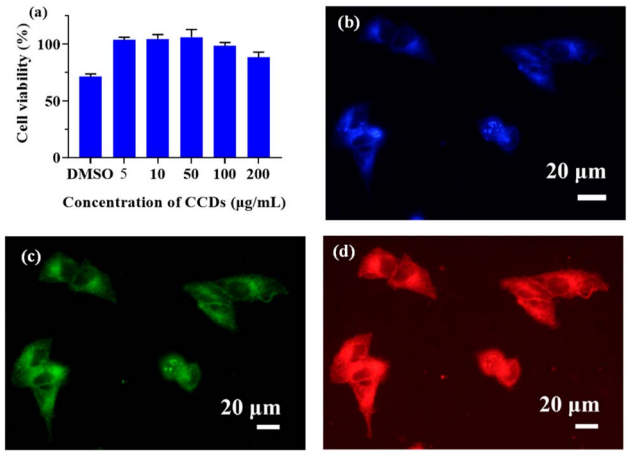

Fig. 8 (a) Cell viability of HepG2 cells in the presence of different concentrations of CCDs with 1% DMSO as the positive control. Confocal microscopy images of CCDs labeled HepG2 cells with different excitation wavelengths at 405 nm (b), 488 nm (c) and 559 nm (d).

prepared CCDs was assayed using the standard CCK-8 method. As shown in Fig. 8a, the average cell viability was close to 100% after the 24 h incubation with CCDs at concentration between 5–100 μg mL^{-1}. As the concentration of CCDs further increased to 200 μg mL^{-1}, the cell viability still remained over 88%. These results suggested that the CCDs showed low toxicity to HepG2 cells and could be potentially employed as a fluorescent probe for cell imaging or other biomedical applications.

For cell imaging, HepG2 cells were incubated with 100 μg mL^{-1} CCDs solution for 2 h, and then observed with confocal laser scanning microscopy. As shown in Fig. 8b–d, there was no obvious change in cell morphology after CDDs treatment. The HepG2 cells treated with CCDs exhibited bright fluorescence (blue, green, and red) when excited at 405 nm, 488 nm and 559 nm, suggesting that the CCDs may have penetrated the cell membrane after 2 h incubation and maintained their fluorescence, thereby labelling the cells. These results suggested that CCDs could be used as fluorescent agents for cell imaging.

4 Conclusions

In summary, novel β-cyclodextrin doped carbon dots (CCDs) were prepared by hydrothermal method at a mild temperature. The β-cyclodextrin-like structure retained under low temperature reaction was, for the first time, used as the isoniazid recognition site for carbon dots. The fluorescence of CCDs can be quenched by isoniazid *via* host–guest recognition through the combined effect of the static and dynamic quenching mechanisms. An isoniazid sensor was constructed and the sensor presented a low detection limit of detection of 0.140 μg mL^{-1} under optimized conditions. The sensor was successfully applied to detect isoniazid in human urine samples with satisfactory recovery (91.1–109.5%). Furthermore, CCDs showed low cytotoxicity to HepG2 cells and it was successfully applied for cell imaging. The present study not only provided a new strategy to enhance quantum yield of CDs, but also expanded the application range of the CDs.

Author contributions

Lu-Shuang Li: conceptualization, methodology, investigation, writing-original draft, funding acquisition. Ying-Xia Zhang: data curation, software. Wei Gong: data curation (cell imaging), writing-review & editing, funding acquisition. Jing Li: conceptualization, supervision, data curation, funding acquisition.

Conflicts of interest

There are no conflicts to declare.

Acknowledgements

The authors gratefully acknowledge the financial support of this research by the Natural Science Foundation of Hainan Province (No. 520QN223), the Starting Research Fund from the Hainan University (No. KYQD(ZR)19106), the financial support of Young Talents Project of TCM Scientific Research of Hubei Provincial Health Commission (No. ZY2021Q025) and the Science and Technology Plan of Xiangyang City (No. 2017YL05).

Notes and references

1 Z. Shekarbeygi, N. Farhadian, M. Ansari, M. Shahlaei and S. Moradi, *Spectrochim. Acta, Part A*, 2020, **228**, 117848.
2 K. Ma, L. Liang, X. Zhou, W. Tan, O. Hu and Z. Chen, *Spectrochim. Acta, Part A*, 2021, **247**, 119097.
3 J. Qin, L. Zhang and R. Yang, *J. Nanopart. Res.*, 2019, **21**, 59.
4 N. Azizi, T. Hallaj and N. Samadi, *Luminescence*, 2022, **37**, 153–160.
5 H. K. Sadhanala, S. Pagidi and A. Gedanken, *J. Mater. Chem. C*, 2021, **9**, 1632–1640.
6 S. Majumdar, U. Baruah, G. Majumdar, D. Thakur and D. Chowdhury, *RSC Adv.*, 2016, **6**, 57327–57334.
7 L.-S. Li, X.-Y. Jiao, Y. Zhang, C. Cheng, K. Huang and L. Xu, *Sens. Actuators, B*, 2018, **268**, 84–92.
8 L.-S. Li, X.-Y. Jiao, Y. Zhang, C. Cheng, K. Huang and L. Xu, *Sens. Actuators, B*, 2018, **263**, 426–435.
9 N. Wang, A.-Q. Zheng, X. Liu, J.-J. Chen, T. Yang, M.-L. Chen and J.-H. Wang, *ACS Appl. Mater. Inter.*, 2018, **10**, 7901–7909.
10 S. Zhu, Q. Meng, L. Wang, J. Zhang, Y. Song, H. Jin, K. Zhang, H. Sun, H. Wang and B. Yang, *Angew. Chem., Int. Ed.*, 2013, **52**, 3953–3957.
11 Y. Huang, N. He, Q. Kang, D. Z. Shen, X. Y. Wang, Y. Q. Wang and L. X. Chen, *Analyst*, 2019, **144**, 6609–6616.
12 H. Y. Lee, P. Y. Chiang, H. J. Wu, T. Y. Wang, T. C. Yang, W. C. Cheng, L. C. Lo and W. S. Liao, *ACS Appl. Nano Mater.*, 2021, **4**, 6852–6860.
13 S. Huang, E. Yang, J. Yao, Y. Liu and Q. Xiao, *Anal. Chim. Acta*, 2018, **1035**, 192–202.
14 Y. Ma, G. Xu, F. Wei, Y. Cen, Y. Song, Y. Ma, X. Xu, M. Shi, M. Sohail and Q. Hu, *Nanotechnology*, 2018, **29**, 145501.

© 2022 The Author(s). Published by the Royal Society of Chemistry

Open Access Article. Published on 21 October 2022. Downloaded on 10/3/2024 7:25:47 AM.
This article is licensed under a Creative Commons Attribution-NonCommercial 3.0 Unported Licence.

15 B. B. Campos, R. Contreras-Caceres, T. J. Bandosz, J. Jimenez-Jimenez, E. Rodriguez-Castellon, J. da Silva and M. Algarra, *Sens. Actuators, B*, 2017, **239**, 553–561.
16 Z. S. Hosseini, A. I. Zad, M. A. Ghiass, S. Fardindoost and S. Hatamie, *J. Mater. Chem. C*, 2017, **5**, 8966–8973.
17 G. Liu, S. Li, M. Cheng, L. Zhao, B. Zhang, Y. Gao, Y. Xu, F. Liu and G. Lu, *New J. Chem.*, 2018, **42**, 13147–13156.
18 Y. Bai, Y. Wang, L. P. Cao, Y. J. Jiang, Y. F. Li, H. Y. Zou, L. Zhan and C. Z. Huang, *Anal. Chem.*, 2021, **93**, 16466–16473.
19 W. Ji, J. L. Yu, J. X. Cheng, L. W. Fu, Z. Y. Zhang, B. W. Li, L. X. Chen and X. Y. Wang, *ACS Appl. Nano Mater.*, 2022, **5**, 1656–1663.
20 X. Y. Wang, J. L. Yu, W. Ji, M. Arabi, L. W. Fu, B. W. Li and L. X. Chen, *ACS Appl. Nano Mater.*, 2021, **4**, 6852–6860.
21 F. Niu, Y.-L. Ying, X. Hua, Y. Niu, Y. Xu and Y.-T. Long, *Carbon*, 2018, **127**, 340–348.
22 Y. Guo, F. Cao and Y. Li, *Sens. Actuators, B*, 2018, **255**, 1105–1111.
23 S. Panda, A. Jadav, N. Panda and S. Mohapatra, *New J. Chem.*, 2018, **42**, 2074–2080.
24 S. Y. Zhao, X. R. Chen, C. X. Zhang, P. T. Zhao, A. J. Ragauskas and X. P. Song, *ACS Appl. Mater. Inter.*, 2021, **13**, 61565–61577.
25 S. Paul, A. Bhattacharya, N. Hazra, K. Gayen, P. Sen and A. Banerjee, *Langmuir*, 2022, **38**, 8829–8836.
26 A. O. Alqarni, S. A. Alkahtani, A. M. Mahmoud and M. M. El-Wekil, *Spectrochim. Acta, Part A*, 2021, **248**, 119180.
27 M. Luo, Y. Hua, Y. Liang, J. Han, D. Liu, W. Zhao and P. Wang, *Biosens. Bioelectron.*, 2017, **98**, 195–201.
28 X. Liao, C. Chen, P. Shi and L. Yue, *Food Chem.*, 2021, **338**, 127769.
29 X. Lu, X. Wen and Z. Fan, *J. Lumin.*, 2020, **221**, 117042.
30 Y. Li, J. Cai, F. Liu, H. Yang, Y. Lin, S. Li, X. Huang and L. Lin, *Talanta*, 2019, **201**, 82–89.
31 A. Cayuela, M. Laura Soriano and M. Valcarcel, *Analyst*, 2016, **141**, 2682–2687.
32 C. Tang, Z. Qian, Y. Huang, J. Xu, H. Ao, M. Zhao, J. Zhou, J. Chen and H. Feng, *Biosens. Bioelectron.*, 2016, **83**, 274–280.
33 X. Lu and Z. Fan, *Spectrochim. Acta, Part A*, 2019, **216**, 342–348.
34 Q. Sun, S. Fang, Y. Fang, Z. Qian and H. Feng, *Talanta*, 2017, **167**, 513–519.
35 J. Xu, Y. Zang, F. Yan, J. Sun, Y. Zhang and C. Yi, *Part. Part. Syst. Charact.*, 2021, **38**, 2100201.
36 M. G. Teixeira, J. V. de Assis, C. G. Soares, M. F. Venancio, J. F. Lopes, C. S. Nascimento Jr, C. P. Anconi, G. S. Carvalho, C. S. Lourenco, M. V. de Almeida, S. A. Fernandes and W. B. de Almeida, *J. Phys. Chem. B*, 2014, **118**, 81–93.
37 I. V. Terekhova and R. S. Kumeev, *Russ. J. Phys. Chem. A*, 2009, **84**, 1–6.
38 L. Tom, C. R. Nirmal, A. Dusthackeer, B. Magizhaveni and M. R. P. Kurup, *New J. Chem.*, 2020, **44**, 4467–4477.
39 Y.-T. Yen, Y.-S. Lin, T.-H. Chen, S.-C. Chyueh and H.-T. Chang, *Sens. Actuators, B*, 2020, **305**, 127441.
40 L. Li, L. Shi, J. Jia, O. Eltayeb, W. Lu, Y. Tang, C. Dong and S. Shuang, *Sens. Actuators, B*, 2021, **332**, 129513.
41 C. Wang, J. Zhou, G. Ran, F. Li, Z. Zhong, Q. Song and Q. Dong, *J. Mater. Chem. C*, 2017, **5**, 434–443.
42 Z. H. Wang, L. Zhang, Y. M. Hao, W. J. Dong, Y. Liu, S. M. Song, S. M. Shuang, C. Dong and X. J. Gong, *Anal. Chim. Acta*, 2021, **1144**, 1–13.
43 S. Hu, R. Tian, Y. Dong, J. Yang, J. Liu and Q. Chang, *Nanoscale*, 2013, **5**, 11665–11671.
44 C. Tang, J. Zhou, Z. Qian, Y. Ma, Y. Huang and H. Feng, *J. Mater. Chem. B*, 2017, **5**, 1971–1979.
45 V. Ramanan, B. Siddaiah, K. Raji and P. Ramamurthy, *ACS Sustainable Chem. Eng.*, 2018, **6**, 1627–1638.
46 J. S. Sidhu, A. Singh, N. Garg and N. Singh, *ACS Appl. Mater. Inter.*, 2017, **9**, 25847–25856.
47 L. Huang and A. E. Tonelli, *Polym. Rev.*, 1998, **38**, 781–837.
48 Z. M. Zhao, Y. Z. Guo, T. Zhang, J. L. Ma, H. M. Li, J. H. Zhou, Z. W. Wang and R. C. Sun, *Int. J. Biol. Macromol.*, 2020, **164**, 4289–4298.
49 Y. Yang, Q. Y. Wei, T. Zou, Y. L. Kong, L. F. Su, D. Ma and Y. D. Wang, *Sens. Actuators, B*, 2020, **321**, 128534.
50 R. Li, W. Wang, M. E.-S. El-Sayed, K. Su, P. He and D. Yuan, *Sens. Actuators, B*, 2021, **330**, 129314.

© 2022 The Author(s). Published by the Royal Society of Chemistry